Heliyon 6 (2020) e03663

Contents lists available at ScienceDirect

Heliyon

journal homepage: www.cell.com/heliyon

Research article

Photocatalytic degradation of methylene blue dye in aqueous solution by $MnTiO_3$ nanoparticles under sunlight irradiation

Suhila Alkaykh [a], Aïcha Mbarek [b,*], Elbashir E. Ali-Shattle [c]

[a] Chemistry Department, School of Basic Sciences, Libyan Academy Tripoli-Libya, Libya
[b] Laboratory of Advanced Materials, National School of Engineers of Sfax, University of Sfax, Tunisia
[c] Chemistry Department, College of Science, Tripoli University, Tripoli, Libya

ARTICLE INFO

Keywords:
Inorganic chemistry
Materials chemistry
$MnTiO_3$
Solar light
Methylene blue dye
Photocatalysis
Nanocrystalline

ABSTRACT

Nanophotocatalyst $MnTiO_3$ powders were synthesized by sol-gel technique and characterized by means of X-ray diffraction (XRD), Fourier transform infrared spectroscopy (FTIR), as well as their thermal behavior has been studied by differential thermal and thermogravimetric analyses (DTA/TGA). Powders morphology was analyzed by means of Transmission electron microscopy (TEM). Effect of various process parameters like amount of photocatalyst, dye concentration, solution pH and irradiation time on the extent of removal of dye were studied in detail. The photo-degradation was relatively higher using lower amount (0.005 g) of semiconductor, reached rate of 75% and 70% after 240 min for mixed $MnTiO_3/TiO_2$ and pure $MnTiO_3$ nanocatalysts. The kinetic model of photocatalytic degradation of MB follows pseudo-first-order kinetic with a high correlation coefficient values ($R^2 > 0.95$). These results underline the use of effective, low-cost and easily available $MnTiO_3$ photocatalyst for the decomposition of pollutants to water under natural sunlight.

1. Introduction

The residual dyes from textile, pharmaceutical or dye intermediates industries are considered non-biodegradable organic pollutants introduced into the natural water resources or wastewater treatment systems [1, 2, 3]. In particular, the discharge of effluents containing dyes into the water environment is undesirable, due to their color which generates toxic products through hydrolysis; oxidation or other chemical reactions in the wastewater phase [3, 4, 5]. At present, the photocatalysis process allows performing the efficient degradation of variety of organic pollutants in aqueous wastes [6, 7, 8, 9, 10]. This process is based on the use of semiconductor materials, which upon activation with suitable light sources give rise to the formation of various reactive species. Among various semiconductor photo-catalysts, the perovskite type ABO_3 oxides (A and B are two cations of different sizes) have received considerable attention for their good abilities towards water splitting and organic pollutant degradation under visible light or UV irradiation [11, 12, 13]. Particularly, manganese titanate $MnTiO_3$ is the most stable perovskite type oxide and a favorable material with strong adsorption in the visible region which appear suitable for photocatalysis applications [14, 15, 16, 17]. However, He *et al.* have reported the photodegradation of aqueous methyl orange on $MnTiO_3$ powder at different initial pH and it was found that this catalyst showed promise for use in many applications in heterogeneous catalysis and decontamination of the environment [16].

The present work reports the photocatalytic degradation of methylene blue (MB) in aqueous solution using $MnTiO_3$ nanoparticles as photocatalyst under sunlight radiation. A comparative photocatalytic activity of $MnTiO_3$ powders, synthesized by the sol-gel process following two methods of preparation, has been investigated. The effects of different operational parameters on the degradation of dye have also been studied along with their reaction kinetics.

2. Experimental methods

2.1. Preparation and characterization of nanocatalyst

$MnTiO_3$ nanopowders were synthesized according to the previously reported sol-gel methods [16, 18].

- Sol-gel method 1 (SG-1): 0.01 mol $MnCl_2.4H_2O$ dissolved into distilled water was reacted with 0.02 mol NaOH to produce $Mn(OH)_2$. Then 0.01 mol of TiO_2 (P-25 powder: mixture of 70% Rutile and 30% Antase) was added to the above solution. The mixed solution was further refluxed for 12 h at 75 °C. The supernatant was then decanted,

* Corresponding author.
E-mail address: mbarekaicha@yahoo.fr (A. Mbarek).

https://doi.org/10.1016/j.heliyon.2020.e03663
Received 13 January 2019; Received in revised form 15 April 2019; Accepted 20 March 2020

and the solid residue was washed three times with distilled water, dried in air at 100 °C for 12 h and calcined in air at 900 °C for 6 h.

- Sol-gel method 2 (SG-2): An appropriate amount of Manganese chloride tetrahydrate $MnCl_4$. $4H_2O$ (0.6 g) was dissolved in distilled water with addition 0.12 mL of nitric acid HNO_3, 1.6 mL acetic acid CH_3COOH and then 1 ml of titanium isopropoxide, $Ti[O(C_3H_7)]_4$ was added to the above mixture and a white precipitate was formed immediately. The mixture was then stirred for 12 h maintaining the temperature at 50 °C. The resulting semi-transparent colloidal suspension solution was evaporated at 80 °C. The obtained powder was dried and treated at 900 °C for 6 h.

The X-ray diffraction (XRD) measurement was carried out at room temperature using a Philips X-Pert Pro diffractometer. The TEM micrographs were obtained on a JEOL 2011 transmission electron microscope with an accelerating voltage of 200 kV. The infrared spectra were recorded with a NICOLET 5700-FTIR spectrometer equipped with an attenuated total reflection (ATR) accessory. Thermoanalytical measurements (TG/DTA) were performed using a SETARAM TG-DTA92 microbalance and the thermograms were recorded between 30 and 1200 °C with a heating rate of 10 °C/min.

2.2. Photocatalytic activity

The photocatalytic activities of pure $MnTiO_3$ and mixed $MnTiO_3$/TiO_2 were tested in five neck pyrex flask type reactor under sunlight irradiation. 0.005 g of the photocatalysts were introduced into the 50 ml aqueous solution of methylene blue ($1 \times 10^{5-}$ M, pH = 6.4). The decomposed dye solutions were centrifuged at 4000 rpm for 10 min and for the measurement of UV-visible absorbance (OPTIMA UV-vis spectrometer SP-3000 Plus). The photo-degradation rate of methylene blue (MB) was calculated by the following Eq. (1) [19]:

$$\text{Degradation } (\%) = \frac{A_0 - A_t}{A_0} \times 100 \quad (1)$$

where A_0 is the absorbance of initial MB; A_t is the absorbance of the solution after illumination at time t. According to first order kinetics reaction, rate constant k (min^{-1}) was determined by using the following relation (2) [20]:

$$\ln\left(\frac{C_t}{C_0}\right) = -kt \quad (2)$$

where C_0 and C_t are concentration at the beginning and at a certain time, t is the irradiation time. Adsorption kinetics investigations were carried out by agitating 50 mL of MB (1×10^{-5} M) dye solution of known initial concentration with 0.005 g of adsorbent prepared by SG-1 and SG-2 routes (pH = 6.4).

3. Results and discussion

3.1. Catalyst characterization

Figure 1(a) and (b) present the XRD patterns of $MnTiO_3$ powders synthesized by the both routes SG-1 and SG-2 respectively. The X-ray diffraction pattern in Figure 1(a) suggests the crystallisation of rhombohedral $MnTiO_3$ phase (JCPDS: 29-0902) [21] along with amount of TiO_2 rutile phase (2θ = 27.59, 33.12, 36.22 and 54.61) (* marked peaks, JCPDS: 78-1508) [22]. The semi quant % of $MnTiO_3$ and TiO_2 are for powder prepared by sol-gel, method 1 (SG-1) are 77.6% and 22.4% respectively. Figure 1(b) shows the XRD pattern of the product synthesized by using Titanium isopropoxide as precursor (SG-2). All the reflection peaks can be indexed to rhombohedral pyrophanite phase $MnTiO_3$ (JCPDS 29-0902). No peaks corresponding to rutile phase are detected in the XRD pattern, which shows the high purity of the product.

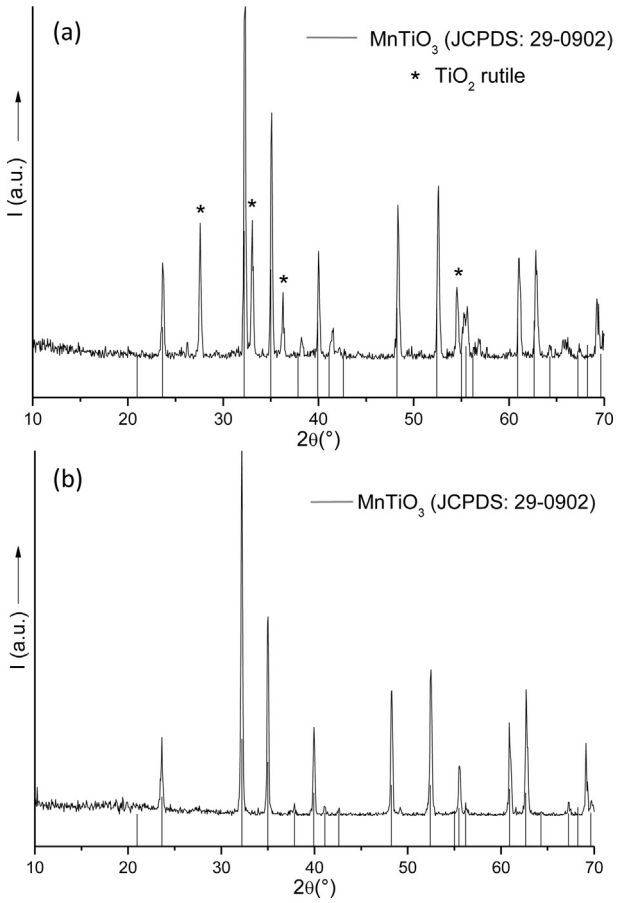

Figure 1. X-ray diffraction pattern for $MnTiO_3$ prepared using (a) Titanium dioxide powder P-25 (SG-1) or (b) Titanium isopropoxide as precursor (SG-2).

The crystallite sizes of the particles were estimated from XRD peak half widths using the Scherrer Eq. (3) [23]:

$$D = \frac{0.9\lambda}{b\cos\theta} \quad (3)$$

where D is the average crystallite diameter, λ is the X-ray wavelength, b is the full width at half maximum (FWHM) of the peak corrected for instrumental broadening and θ is the Braggs' angle. The calculated values average particle diameters for $MnTiO_3$ powders synthesized by sol-gel method SG-1 and SG-2 were approximately 29.2 and 35.5 nm respectively.

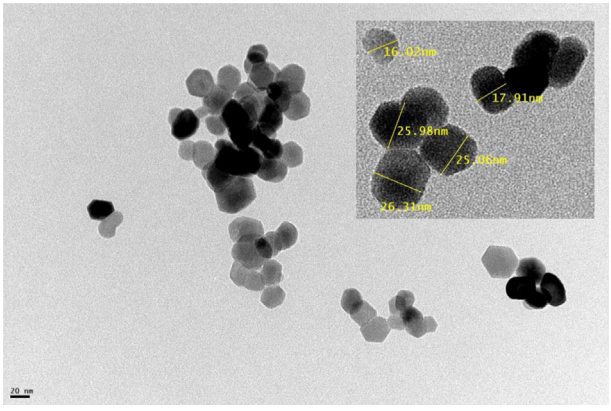

Figure 2. TEM picture of $MnTiO_3$ nanopowder prepared by sol-gel method 2 and calcined at 900 °C.

The TEM micrographs of $MnTiO_3$ sample are illustrated in Figure 2. It is found that the nanoparticles possess almost spherical shape. These spherical nano assemblies are discrete and well defined with limited aggregation and a narrow size distribution ranging between 15–35 nm. The result agrees well with that of the XRD analysis.

Room temperature IR/ATR spectra recorded for $MnTiO_3$ samples prepared by both synthesis routes (SG-1 and SG-2) and measured in the range of 400–2000 cm^{-1} spectral region are shown in Figure 3. Their spectra are characterized with main absorption bands of $MnTiO_3$. The bands centered at 407, 494, and 656 cm^{-1} were attributed to the Ti–O bond vibrations. The bands at 407 and 494 cm^{-1} can be assigned to Mn–O–Ti and O–Ti–O vibrational modes, respectively [24]. The band centered around 657 cm^{-1} observed in SG-1 sample can be also attributed to corresponding Ti–O modes of crystalline rutile TiO_2. The band appearing at 970 cm^{-1} is due to Mn–O bonds for SG-2 sample [25].

To investigate the domains of stability and decomposition of $MnTiO_3$ treated at 900 °C, Thermogravimetric and differential thermal analysis (TGA and DTA) of samples prepared by SG-1 and SG-2 methods were performed. The thermograms in Figure 4 show no thermal effects accompanied by mass losses. The endothermic peak between 80 °C and 250 °C observed for both synthesis sol-gel routes can be attributed to dehydration of water molecules. In the temperature range of 250–450 °C, no weight loss was exhibited, that proves the absence of hydroxyl groups and/or organic residues such as alkoxy groups in the powder of $MnTiO_3$. It showed that no significant changes were observed both in DTA and TGA curves even up to 1200 °C. As we expected, the thermal stability of $MnTiO_3$ was improved effectively. For the compound prepared by sol-gel method 1, were titanium dioxide powder used as starting precursor, a slight endothermic effect is identified accompanied with low mass loss observed around 1000 °C (Figure 4(a)). From the foregoing XRD characterization, the presence of titanium dioxide TiO_2 was observed in the calcined powder SG-1 at 900 °C. According to these observations, we can hypothesize that the endothermic peak around 1000 °C corresponds to the decomposition or loss of TiO_2 rutile phase.

3.2. Photocatalytic degradation of MB

To understand photocatalytic degradation of methylene blue dye using semi-conductor $MnTiO_3$ nanoparticles as catalyst, we studied the influence of several factors on the degradation process including contact time, initial concentration of dye, photocatalyst loading, solution pH and nature of light source.

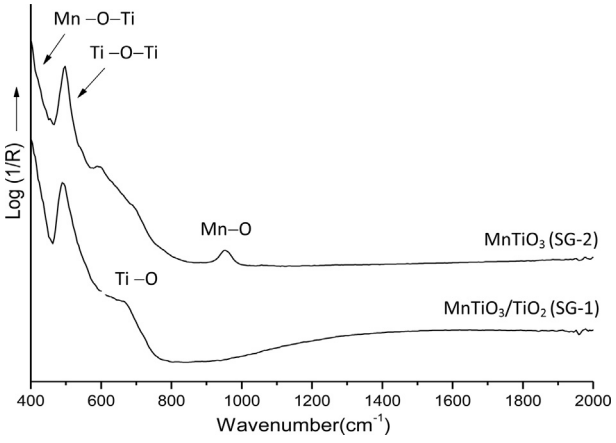

Figure 3. IR/ATR spectra of samples prepared by SG-1 and SG-2 methods, after heating at 900 °C.

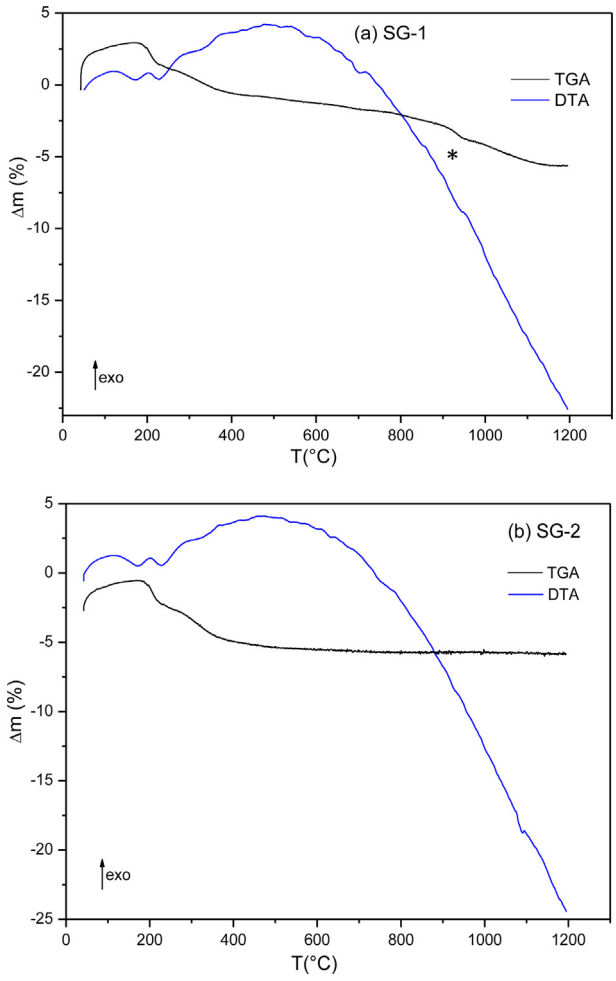

Figure 4. TG-DTA curves of the as-synthesized nanopowders obtained by (a) SG-1 and (b) SG-2 methods.

- **Effect of contact time**

Adsorption of methylene blue on $MnTiO_3$ nanocatalyst surface, obviously, is a function of the contact time, which is corresponding to the

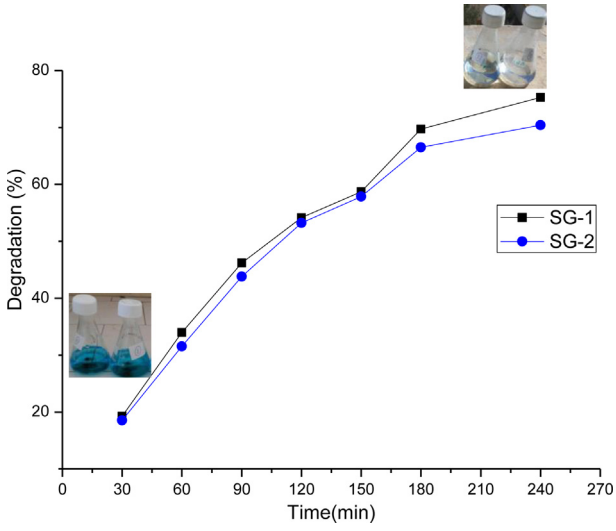

Figure 5. Effect of contact time on MB dye removal onto $MnTiO_3$-TiO_2 (SG-1) and (b) $MnTiO_3$ (SG-2) catalysts.

time of adsorption, or the state of saturation of the absorbant surface by the absorbate (dye). Figure 5 presents the effect of contact time on the removal of methylene blue using 0.005 g of catalysts in aqueous solution. The result show that the catalysis of photodecomposition of methylene blue (MB) occurs. It was observed as shown in Figure 5, the efficiency of MB decolorization using the individual $MnTiO_3$ catalyst (SG-2) is substantially identical as compared with the mixture $MnTiO_3/TiO_2$ catalyst (SG-1). However, for the mixed photocatalyst $MnTiO_3/TiO_2$, the degradation was quite high (75%) as compared with the pure $MnTiO_3$ nanoparticule (70%) after 240 min irradiation under sunlight.

- **Effect of the dye concentration**

The influence of the initial dye concentration on the decolorization of MB was studied under sunlight irradiation by varying the initial dye concentrations from 2×10^{-6} M to 1.5×10^{-5} M in the presence of 0.005 g of photocatalyst. From Figure 6, it can be seen that the removal efficiency of dye increases with increasing initial concentration of the dye until 1×10^{-5} M after 240 min irradiation time. The adsorption capacity is higher at lower concentration because of the higher availability of more active sites for MB molecules to be adsorbed on the surface $MnTiO_3$ photo-catalyst. When dye concentration increases, number of dye molecules adsorbed on catalyst surface increases. Increasing the dye concentration also caused the dye molecules to adsorb light and the photons never reached $MnTiO_3$ surface; finally, it causes reduced efficiency of dye removal [26, 27]. Thus, the photodegradation of MB was found better at low concentration, i.e $[MB]_o \leq 1 \times 10^{-5}$ M.

- **Effect of catalyst dose**

The degradation percentage of MB dye under visible light irradiation by different amounts of photo catalyst were used (0.005 g–0.04 g), was examined. As it can be seen in Figure 7, the rate of photodegradation was higher using lower amount (0.005 g) of semiconductor, 76% of MB degradation for $MnTiO_3/TiO_2$ catalyst obtained by SG-1 (Figure 7(a)) and 62.5% of MB degradation for $MnTiO_3$ catalyst prepared by SG-2 (Figure 7(b)). Whereas, the presence of TiO_2 improved the reaction photodegradation of MB dye. It has been reported that TiO_2 represent a good photocatalytic activity for the decomposition of organic pollutants [28, 29]. Beyond 0.005 g of $MnTiO_3$ nanoparticle, the percentage degradation of MB dye increases only slightly up to 0.04 g. These observations can be rationalized both in terms of availability of active sites on $MnTiO_3$ surface and the light penetration of photo-activating light into the system [30]. At higher catalyst loading may be due to the deactivation of activated molecules by collision with ground state catalysts, thus reducing the rate of reaction [31].

- **Effect of pH**

Another important parameter in the photocatalytic reactions is the pH of the solution. It has a significant effect on the surface charge of the photocatalyst [32]. The pH of methylene blue solution was adjusted by adding HCl or NaOH (1 M). The effect of the solution pH on the rate of photocatalytic degradation was investigated within the range of 2–9 at constant dye concentration (1×10^{-5} M) and catalyst amount 0.005g/50mL $MnTiO_3/TiO_2$ (Figure 8(a)) or $MnTiO_3$ (Figure 8(b)). The removal of dye by adsorption onto nanosized $MnTiO_3$ was found to be slow at the initial period of contact time, and then to become rapid with the increase of contact time. An increase in the degradation of MB dye was observed with increasing the pH from 2 to 9. The percentage of removal increases from 15% in pH = 2–60% in pH = 9 of the solution, for the two nanosized photocatalytic materials prepared by SG-1 and SG-2 routes.

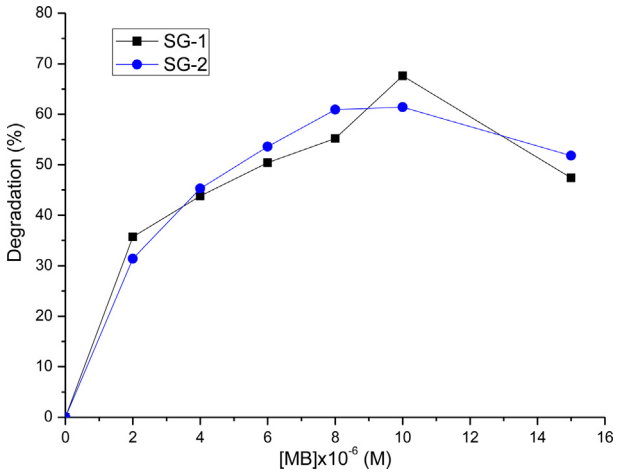

Figure 6. Effect of initial MB dye concentration on the adsorption of MB onto nanosizes catalysts, prepared by SG-1 and SG-2 methods.

- **Effect of light intensity**

Intensity of light and the effect of the radiation wavelength both have affect on the rate of photo-degradation of pollutants [33, 34, 35]. The light intensity was varied by changing the source of irradiation. For that, two kinds of lamps 10 W UV-C ($\lambda = 254$ nm) and 100 W UV-A ($\lambda = 356$ nm) were used. Figure 9 illustrates the effect of the variation of light intensity on the degradation of MB dye. From the observed data, it is

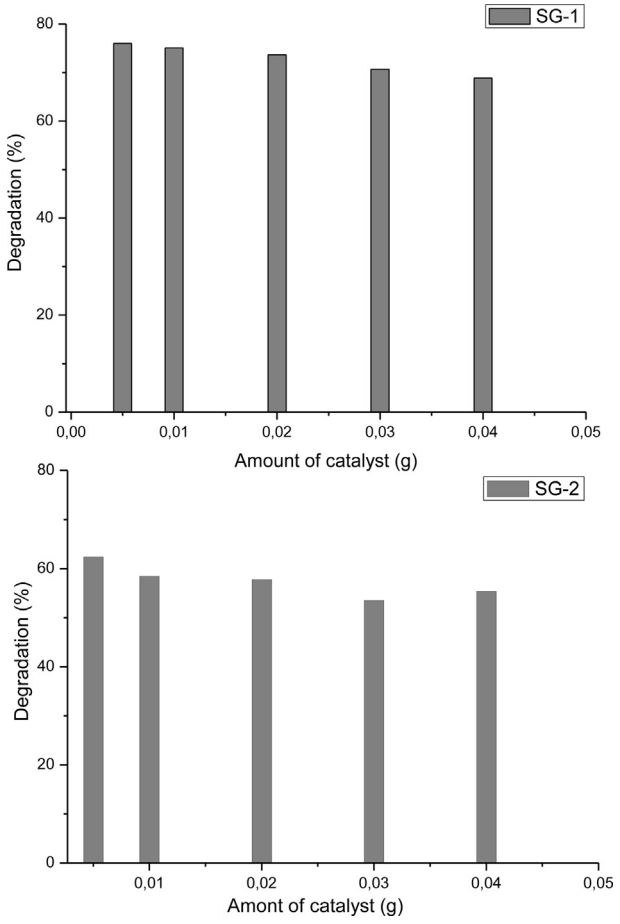

Figure 7. Effect of $MnTiO_3$ catalyst dose prepared by (a) SG-1 and (b) SG-2 method on the methylene blue removal.

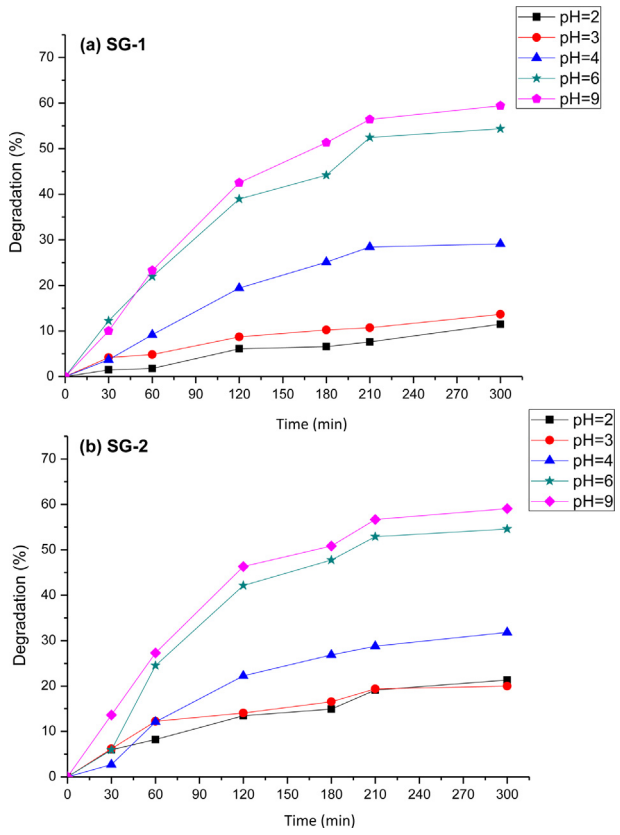

Figure 8. Influence of pH on the photocatalytic degradation onto catalysts prepared by (a) SG-1 and (b) SG-2 methods.

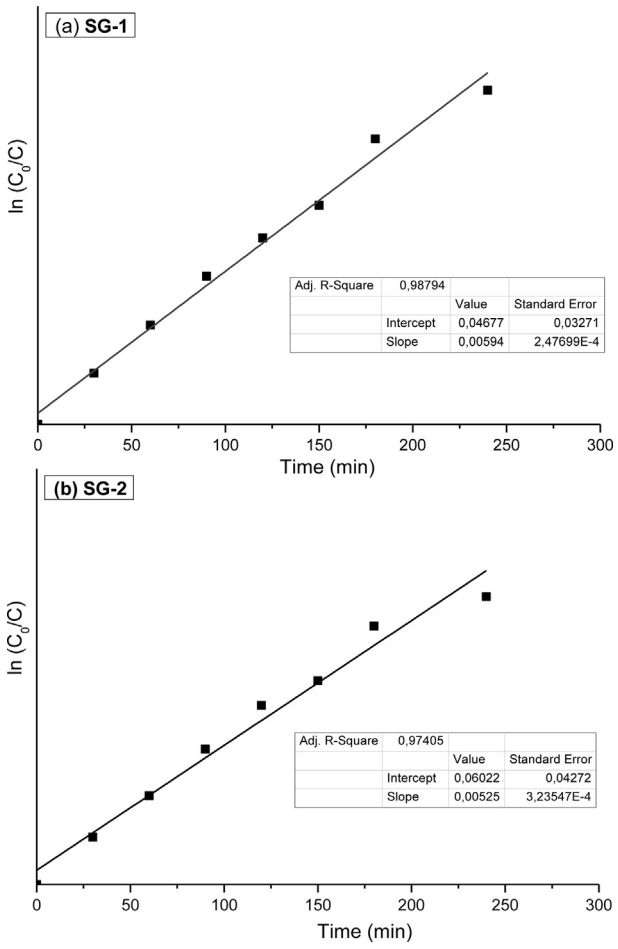

Figure 10. Pseudo-first-order kinetics plots of MB adsorption on with (a) $MnTiO_3$-TiO_2 (SG-1) and (b) $MnTiO_3$ (SG-2).

evident that the degradation of methylene blue using solar light irradiation was more efficient than that with artificial UV light irradiation. The percent (%) of degradation of methylene blue was significantly improved with UV-C radiation compared to UV-A radiation. An increase in light intensity did not result in any significant corresponding increase in the degradation efficiency. This probably means that the optimum number of photons required for effective photocatalytic degradation was attained under UV 10 W. Therefore, an increase in photon number under UV 100 W did not produce any major change in the degradation efficiency [36, 37].

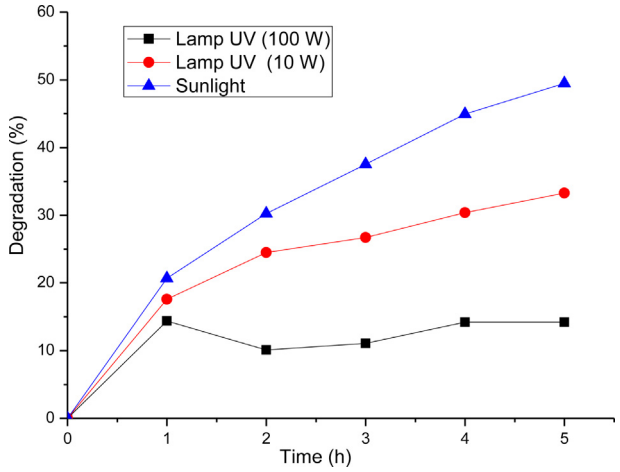

Figure 9. Effect of solar/UV light source on the degradation of MB dye.

- **Adsorption kinetics**

The kinetics of an adsorption process provides information about the mechanism of adsorption. The pseudo-first order kinetic equation given by the Langmuir-Hinshelwood model at low initial concentrations [16] was tested. Figures. 10(a) and (b) show the reaction kinetics of MB degradation in the presence of pure $MnTiO_3$ (obtained by SG-2 route) and $MnTiO_3$-TiO_2 (prepared by SG-1 synthesis). By plotting $\ln(C_0/C)$ vs t, a straight line was obtained. From the graphs, it is seen that the photocatalytic methylene blue dye degradation follow the first order-kinetics as the correlation constant for the fitted line to be $R^2 > 0.95$. A good correlation to the first order reaction kinetics ($R^2 = 0.988$ for $MnTiO_3$--TiO_2 and $R^2 = 0.974$ for $MnTiO_3$) was found. The calculated pseudo-first-order rate constants of $MnTiO_3$-TiO_2 and pure $MnTiO_3$ are 5.96 10^{-3} min^{-1} and 5.25 10^{-3} min^{-1} respectively. The results further demonstrated that $MnTiO_3$ photocatalyst exhibits good photo-reactivity which corroborates the corresponding degradation efficiency.

4. Conclusions

In summary, pure $MnTiO_3$ or mixed $MnTiO_3/TiO_2$ nanoparticules have been successfully prepared by sol-gel method. The structure and morphology of these nanoparticles were studied using X-ray diffraction

and high resolution transmission electron microscopy analysis. The particles are in the average crystallite size range of 20–30 nm. The experiments of degrading MB confirmed that the obtained catalysts can perform significant photocatalytic activity even if it is irradiated by solar light. Therefore, the $MnTiO_3$ nanoparticule is a good candidate in the treatment of industrial wastewater to eliminate organic pollutants, which cause severe threat to environment.

Declarations

Author contribution statement

Suhila Alkaykh: Conceived and designed the experiments; Performed the experiments; Analyzed and interpreted the data; Contributed reagents, materials, analysis tools or data.

Aïcha Mbarek: Performed the experiments; Analyzed and interpreted the data; Contributed reagents, materials, analysis tools or data; Wrote the paper.

Elbashir E. Ali-Shattle: Analyzed and interpreted the data.

Funding statement

This research did not receive any specific grant from funding agencies in the public, commercial, or not-for-profit sectors.

Competing interest statement

The authors declare no conflict of interest.

Additional information

No additional information is available for this paper.

References

[1] D.G. Crosby, Environmental Toxicology and Chemistry, Oxford University Press, New York, 1998.
[2] E. Forgacs, T. Crestile, G. Oros, Removal of synthetic dyes from waste water. A review, Environ. Int. 30 (2004) 953–971.
[3] I.M. Banat, P. Nigam, D. Singh, R. Marchant, Microbial decolorization of textile-dye-containing effluents: a review, Bioresour. Technol. 58 (1996) 217–227.
[4] R. Kant, Textile dyeing industry an environmental hazard, Univ. Inst. Fashion Tech. 4 (2012) 22–26.
[5] H. Zollinger, Synthesis, properties of organic dyes and pigments. Color Chemis- Try, VCH Publishers, New York, USA, 1987, pp. 92–102.
[6] M.R. Hoffmann, S.T. Martin, W. choi, D.W. Bahnemann, Environmental applications of semiconductor photocatalysis, Chem. Rev. 95 (1995) 69–96.
[7] D.S. Bhatkhande, V.G. Garkar, A.A.C.M. Beenackers, Surfactant-assisted sol-gel synthesis of TiO_2 with uniform particle size distribution, J. Chem. Technol. Biotechnol. 77 (2001) 102–116.
[8] A.A. Hauas, H.A. Lachheb, K.A. Mohamed, E.A. Elaloui, C. Guillard, J.M. Herrmann, Photocatalytic degradation pathway of methylene blue in water, Appl. Catal. B31 (2001) 145–157.
[9] C. Mei Ling, A.R. Mohamed, S. Bhatia, Performance of photocatalytic reactors using immobilized TiO_2 film for the degradation of phenol and methylene blue dye present in water stream, Chemosphere 57 (2004) 547–554.
[10] R. Jain, S. Shirkarwar, Photocatalytic removal of hazardous dye cyanosine from industrial waste using titanium dioxide, J. Hazard Mater. 152 (2008) 216–220.
[11] N. Labhasetwar, G. Saravanan, S.K. Megarajan, N. Manwar, R. Khobragade, P. Doggali, F. Grasset, Perovskite-type catalytic materials for environmental applications, Sci. Technol. Adv. Mater. 16 (2015) 36002–36015.
[12] J. Shi, L. Guo, ABO_3-based photocatalysts for water splitting, Prog. Nat. Sci. Mater. 22 (2012) 592–615.
[13] P. Kanhere, Z. Chen, A review on visible light active perovskite-based photocatalysts, Molecules 19 (2014) 19995–20022.
[14] W. Dong, D. Wang, L. Jiang, H. Zhu, H. Huang, J. Li, H. Zhao, C. Li, B. Chen, G. Deng, Synthesis of F doping $MnTiO_3$ nanodiscs and their photocatalytic property under visible light, Mater. Lett. 98 (2013) 265–268.
[15] K.N. Bae, S.I. Noh, H.J. Ahn, T.Y. Seong, Effect of $MnTiO_3$ surface treatment on the performance of dye-sensitized solar cells, Mater. Lett. 96 (2013) 67–70.
[16] H.Y. He, W.X. Dong, G.H. Zhang, Photodegradation of aqueous methyl orange on $MnTiO_3$ powder at different initial pH, Res. Chem. Intermed. 36 (2010) 995–1001.
[17] M. Enhessari, A. Parviz, E. Karamali, K. Ozaee, Synthesis, characterisation and optical properties of $MnTiO_3$ nanopowders, J. Exp. Nanosci. 7 (2012) 327–335.
[18] L.G.J. de Haart, A.J. de Vries, G. Blasse, Photoelectrochemical properties of $MgTiO_3$ and other titanates with the ilmenite structure, Mater. Res. Bull. 19 (1984) 817–824.
[19] X. Zhang, G. Zhou, H. Zhang, C. Wu, H. Song, Characterization and activity of visible light–driven TiO_2 photocatalysts co-doped with nitrogen and lanthanum, Transition Meter. Chem. 36 (2011) 217–222.
[20] K. Vasanth Kumar, K. Porkodi, A. Selvaganapathi, Constrain in solving Langmuir-Hinshelwood kinetic expression for the photocatalytic degradation of Auramine O aqueous solutions by ZnO catalyst, Dyes Pigments 75 (2007) 246–249.
[21] R.P. Liferovich, R.H. Mitchell, Rhombohedral ilmenite group nickel titanates with Zn, Mg, and Mn: synthesis and crystal structures, Phys. Chem. Miner. 32 (2005) 442–449.
[22] A.M. Selman, Studies on the influence of growth time on the rutile TiO_2 nanostructures prepared on Si substrates with fabricated high-sensitivity and fast-response p-n heterojunction photodiode, Am. J. Nano Res. Appl. 4 (3) (2016) 23–32.
[23] P. Scherrer, Nanoscience and the scherrer equation versus the scherrer-gottingen equation, Nach. Ges. Wiss. Göttingen 26/9 (1918) 98–100.
[24] O. Harizanov, T. Ivanova, A. Harizanova, Study of sol–gel TiO_2 and TiO_2–MnO obtained from a peptized solution, Mater. Lett. 49 (3/4) (2001) 165–171.
[25] Y.K. Sharma, M. Kharkwal, S. Uma, R. Nagarajan, Synthesis and characterization of titanates of the formula $MTiO_3$ (M = Mn, Fe, Co, Ni and Cd) by co-precipitation of mixed metal oxalates, Polyhedron 28 (3) (2009) 579–585.
[26] Z. Mengyue, C. Shifu, T.C. Yaowu, Photocatalytic degradation of organophosphous pesticides using thin films of TiO_2, J. Chem. Technol. Biotechnol. 64 (1995) 339–344.
[27] L. Ming, Treatment of dye aqueous solution by UV/TiO_2 process with applying bias potential, Water Sci. 36 (2000) 106–189.
[28] C. Liu, R. Li, W. Zhang, Adsorption property and photocatalytic activity of sol-gel prepared porous TiO_2 using PEG1000 as template, Appl. Mech. Mater. 48–49 (2011) 153–156.
[29] J. Yao, Y. Bai, N. Chen, M. Takahashi, T. Yoko, Sol-gel preparation, characterization, and photocatalytic activity of macroporous TiO_2 thin films, J. Am. Ceram. Soc. 94 (4) (2011) 1191–1197.
[30] R.W. Matthews, Process Engineering for pollution control and waste minimization, Water Res. 24 (1990) 653–660.
[31] J.M. Herrmann, Heterogeneous photocatalysis: an Emerging discipline involving multiphase systems, Catal. Today 24 (1-2) (1995) 157–164.
[32] M.M. Haque, D. Bahnemann, M. Muneer, Photocatalytic degradation of organic pollutants: mechanisms and kinetics photocatalytic degrad, Org. Pollut. Mech. Kinet. 3 (2012) 294–326.
[33] S. Ahmed, M.G. Rasul, W.N. Martens, R.J. Brown, M.A. Hashib, Heterogeneous photocatalytic degradation of phenols in wastewater: a review on current status and developments, Desalination 261 (1-2) (2010) 3–18.
[34] G.L. Puma, P.L. Yue, Effect of the radiation wavelength on the rate of photocatalytic oxidation of organic pollutants, Ind. Eng. Chem. Res. 41 (2002) 5594–5600.
[35] S. Kaneco, M.A. Rahman, T. Suzuki, H. Katsumata, K. Ohta, Optimization of solar photocatalytic degradation conditions of bisphenol A in water using titanium dioxide, J. Photochem. Photobiol. A 163 (2004) 419–424.
[36] W. Wilson Anku, S. Osei-Bonsu Oppong, S. Kumar Shukla, P. Penny Govender, Comparative photocatalytic degradation of monoazo and diazo dyes under simulated visible light using Fe^{3+}/C/S doped-TiO_2 nanoparticles, Acta Chim. Slov. 63 (2016) 380–391.
[37] K.M. Reza, A. Kurny, F. Gulshan, Parameters affecting the photocatalytic degradation of dyes using TiO_2: a review, Appl. Water Sci. 7 (2017) 1569–1578.